doi:10.2533/chimia.2007.175 CHIMIA **2007**, *61*, No. 4

Chimia 61 (2007) 175–178
© Schweizerische Chemische Gesellschaft
ISSN 0009–4293

Structure Sensitivity of Palladium-Catalyzed Liquid-Phase Alcohol Oxidation. A Combined *in situ* ATR-IR and Selective Site Blocking Study

Davide Ferri[§a], Cecilia Mondelli[b], Frank Krumeich[a], and Alfons Baiker*[a]
[§]SCS Poster Prize Winner

Abstract: Knowledge of the structure of active sites is a prerequisite for the rational design of solid catalysts. *In situ* attenuated total reflection infrared (ATR-IR) spectroscopy combined with site selective blocking by CO and isotope labeling allowed us to discriminate the different sites involved in the liquid-phase oxidation of benzyl alcohol on Pd/Al_2O_3. The main reaction, the oxidative dehydrogenation of the alcohol to the corresponding aldehyde, showed only little dependence on structure and occurred on all exposed Pd faces, whereas the undesired product decarbonylation occurred preferentially on hollow sites on Pd (111) planes. Similar ATR-IR studies on a corresponding Bi-promoted Pd/Al_2O_3 catalyst showed virtually no adsorbed CO during dehydrogenation indicating that the sites on Pd (111) planes are blocked by selective deposition of Bi. Thus the improved selectivity of the promoted Pd-Bi/Al_2O_3 used industrially can be traced to the selective blocking of active decarbonylation sites on Pd(111) by Bi.

Keywords: Active sites · Alcohol oxidation · ATR-IR spectroscopy · Bi promotion · Structure sensitivity

Introduction

The aerobic liquid-phase oxidation of alcohols is an example of a relevant industrial catalytic process where the use of single crystals combined with UHV techniques contributed greatly to unravel fundamental aspects of the reaction mechanism. The reaction occurs *via* an oxidative dehydrogenation taking place on metallic Pd[1]. Recent *in situ* spectroscopic studies on commercial Pd/Al_2O_3 catalysts, including attenuated total reflection infrared (ATR-IR) spectroscopy[2,3] and X-ray absorption spectroscopy (XAS),[4] provided unique information on the state of the metal surface during reaction together with the observation of the complex reaction mechanism in which metal particles are involved. The molecular structure of the alcohol allows for a number of side reactions running parallel to the main alcohol dehydrogenation reaction, thus revealing that the catalyst surface is composed of different active sites enabling one (or more) specific reaction(s).

Attenuated Total Reflection Infrared Spectroscopy

Infrared spectroscopy is suited to follow surface species and processes on a heterogeneous catalyst especially under UHV and gas-phase conditions. Understanding the nature of the adsorbates evolving during reaction greatly improves the level of knowledge on reaction mechanisms at surfaces. However, when the catalyst operates in a liquid environment, the information from the surface is typically obscured by the strong signals of the solution. In such cases, extrapolation of UHV or gas-phase data to the liquid phase is often connected with great uncertainty. This limitation can be circumvented using ATR-IR spectroscopy.[5] The theory of total internal reflection predicts that the infrared radiation penetrates into the liquid medium after propagation in an optically transparent medium (internal reflection element, IRE; *e.g.* ZnSe) by few tens of a micron (penetration depth, d_p). When the liquid medium absorbs the infrared radiation, an (ATR-)IR spectrum is obtained. In contrast to common reflection techniques, the infrared radiation does not travel through the liquid film before impinging on the sample therefore limiting the absorption from the liquid medium. For application in liquid-phase heterogeneous catalysis[6] a catalytic material can be deposited on the IRE and in the path of the infrared radiation as schematically shown in Fig. 1 so that species evolving on the catalyst surface can be preferentially monitored.

Here, ATR-IR spectroscopy is used to discriminate active sites exposed on a technical Pd/Al_2O_3 catalyst during the liquid-phase oxidative dehydrogenation of benzyl alcohol (Fig. 1) and simultaneously to probe the catalyst surface during reaction and the reaction progress. The sites active for the desired dehydrogenation reaction as well as those catalyzing the undesired decarbonylation of the product are identified using a combined approach including selective site blocking by CO adsorption and isotope labeling. The assignment of active sites is strongly supported by analysis of the species formed on promoted Pd-Bi/Al_2O_3, an industrially relevant catalyst for this type of reactions.

---

*Correspondence: Prof. Dr. A. Baiker[a]
Tel.: + 41 44 632 3153
Fax: + 41 44 632 1163
E-Mail: baiker@chem.ethz.ch
[a]Institute for Chemical and Bioengineering
ETH Zurich, HCI
Wolfgang-Pauli-Strasse 10
CH-8093 Zurich
[b]Dipartimento di Chimica Inorganica, Metallorganica e Analitica
Università di Milano
Via Venezian 21
I-20133 Milano

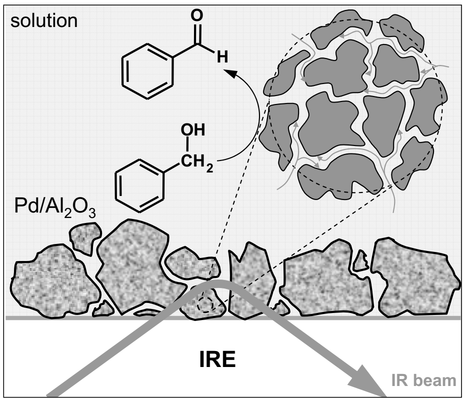

Fig. 1. The principle of ATR-IR spectroscopy and the practical example: the liquid-phase oxidation of benzyl alcohol on Pd/Al_2O_3

Experimental

ATR-IR measurements were carried out using a stainless steel reactor cell[7] mounted in a Bruker Optics Equinox 55 spectrometer equipped with a MCT detector. A suspension containing 4 mg of the 5 wt.% Pd/Al_2O_3 (Johnson Matthey[8]) or of the 0.9 wt.% Bi–5 wt.% Pd/Al_2O_3[4] in water was allowed to dry on the IRE (ZnSe, 45° bevel, 52 × 20 × 2 mm). Benzyl alcohol oxidation was monitored at 50 °C first during contact of the catalyst(s) with an Ar-saturated solution of the alcohol in cyclohexane (20 mM). Then Ar was replaced by air in the same solution without interrupting the liquid flow. Before reaction, the catalyst coating was contacted with H_2-saturated solvent for about 20 min. This treatment affords reduced Pd.[4] In the case of pre-equilibration of the Pd/Al_2O_3 with CO, after catalyst reduction (H_2-saturated solvent, 50 °C, 20 min) CO-saturated cyclohexane was admitted to the ATR-IR cell for about one hour. Then the flow was switched to the Ar-saturated solution of benzyl alcohol (or ^{13}C-benzyl alcohol).

Results and Discussion

Oxidative Dehydrogenation of Benzyl Alcohol

Fig. 2 shows the ATR-IR spectra observed when flowing a solution of benzyl alcohol over reduced Pd/Al_2O_3 under dehydrogenation (Ar) and oxidative (air) conditions.[3] Beside formation of benzaldehyde (signal at 1713 cm^{-1}, *ca.* 4% yield), decomposition of the product to CO (1853 cm^{-1}) and hydration of benzaldehyde to adsorbed benzoate species (signals below 1600 cm^{-1}) occurred as indicated by the infrared signals observed on the catalyst surface under dehydrogenation conditions (alcohol and inert gas). The catalytic activity increased by a factor 3–4 (*ca.* 15% yield) with respect to the dehydrogenation when oxygen was added to the feed yielding also a higher amount of product decarbonylation on Pd. The enhanced formation of benzoate species and of surface water suggests that the catalyst deactivates under prolonged exposure to oxygen. Comparison of the signals of adsorbed CO obtained under dehydrogenation conditions (Fig. 2a) and after adsorption of CO (Fig. 2c) on the reduced catalyst indicates that only specific sites are occupied by CO during benzyl alcohol oxidation on Pd. Nevertheless, the dehydrogenation reaction occurs even in the case of site blocking by CO.

The knowledge of the morphology of the metal particles is crucial to obtain information on the active sites. High resolution TEM indicates that pristine Pd particles are nearly round and 3–4 nm in size with defined (111) and (100) crystalline planes (Fig. 2d)[8] that are not affected upon reduction under bubbling hydrogen in cyclohexane. The ATR-IR spectrum of CO adsorbed on Pd/Al_2O_3 (Fig. 2c) indicates the presence of (100) planes and defect sites (edges, corners; signals at 1968 cm^{-1} for bridge CO and at 2074 and 2050 cm^{-1} for on-top CO), and of hollow sites on (111) planes (low energy shoulder of the signal at 1968 cm^{-1})[9]. This assignment is important for the determination of the active metal sites.

Active Metal Sites

CO originating from decarbonylation of benzaldehyde peaks at 1853 cm^{-1} with a number of shoulders during the liquid-phase oxidation of benzyl alcohol on Pd/Al_2O_3 (Fig. 2a). According to the assignment made for adsorbed CO, the low frequency of the signal indicates that during dehydrogenation CO occupies predominantly hollow sites on (111) planes. This assignment agrees quite well with the preferential adsorption of CO on (111) faces of well-defined Pd nanoparticles contaminated by carbon deposits upon exposure to methanol[10] and with the selective perturbation of the vibration of CO adsorbed on step sites by adsorbed Xe.[11]

The ATR-IR spectra show that upon admission of the alcohol solution saturated with Ar on the Pd/Al_2O_3 catalyst pre-equilibrated with CO (Fig. 3a) the signal at 2074 cm^{-1} is quickly attenuated and the signal at 1968 cm^{-1} rapidly shifts to *ca.* 1950 cm^{-1} and is enhanced. This is likely due to disruption of CO dipole–dipole interactions induced by benzyl alcohol. After few min-

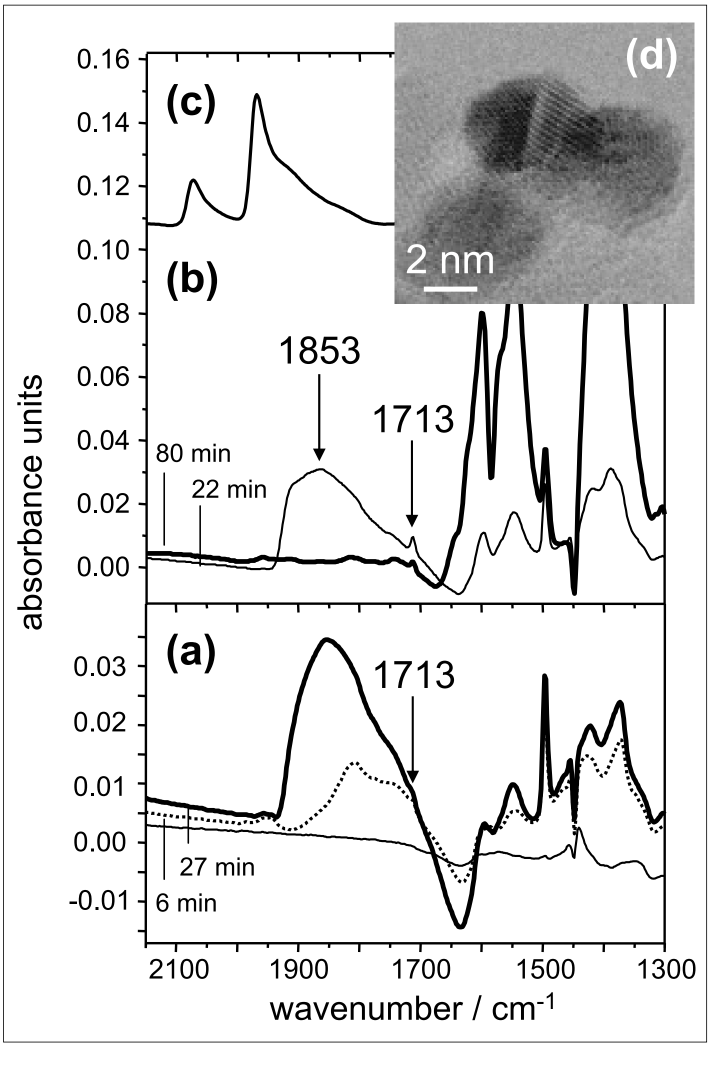

Fig. 2. ATR-IR spectra of a solution of benzyl alcohol on reduced Pd/Al_2O_3 under (a) inert (Ar) and (b) oxidative (air) conditions. (c) Spectrum of CO adsorbed on Pd/Al_2O_3 reduced at 50 °C in flowing H_2-saturated cyclohexane. (d) High resolution transmission electron microscopy (HR-TEM) of the pristine Pd/Al_2O_3 catalyst exposing (111) and (100) planes.[8] Conditions: $C_{alcohol}$ = 20 mM; 4 mg catalyst; cyclohexane solvent; 50 °C; liquid flow rate = 0.6 ml/min.

utes on stream the intensity of the latter signal starts to slowly decrease and the signal shifts by *ca.* 30 cm^{-1}, whereas its low energy flank gains intensity. Catalytic activity monitored by the appearance of the signal at 1713 cm^{-1} of dissolved benzaldehyde is observed only when the signal originally at 1968 cm^{-1} is suddenly consumed (Fig. 3d). At this point a broad CO signal extends between 1950 and 1700 cm^{-1}, which has no equivalent signal in Fig. 2a but resembles the CO feature of Fig. 2c. Benzaldehyde formation under dehydrogenation conditions (absence of oxygen) clearly occurs when CO is completely removed from bridge sites (defects and (100) planes). CO adsorbed in the on-top geometry on corner sites (2074 cm^{-1}) does not appear strictly related to the catalytic activity, since these sites are liberated almost immediately. On the contrary, the on-top geometry on edge sites (*ca.* 2050 cm^{-1}) follows a similar trend to the signal at 1968 cm^{-1}.

Fig. 3 also shows that what remains on Pd after reaction ignition is CO strongly adsorbed predominantly on (111) planes. However, this CO does not originate from benzaldehyde decarbonylation as Fig. 2 would suggest, but is residual CO from the pre-equilibration of Pd/Al$_2$O$_3$ with CO. This is demonstrated in an equivalent experiment to that shown in Fig. 3a with benzyl alcohol labeled with ^{13}C at the methylene group (Fig. 3b). This approach is based on the fact that dehydrogenation of this alcohol should afford benzaldehyde labeled at the carbonyl carbon atom and the decarbonylation of this product should provide ^{13}CO. Owing to the isotope effect the signals of carbonyl-containing species evolving during oxidative dehydrogenation of labeled benzyl alcohol are red-shifted compared to Fig. 2, but the surface chemistry remains obviously identical (Fig. 3c). After pre-equilibration of Pd/Al$_2$O$_3$ with CO and admission of the solution of ^{13}C-benzyl alcohol, no ^{13}CO is detected when ^{13}C-labeled benzaldehyde appears and the shape of the remaining CO signal is identical to that obtained with benzyl alcohol (Fig. 3a) and to that shown in Fig. 2.

The selective site blocking achieved using CO provides evidence that benzyl alcohol displaces CO from bridge sites (defects and (100) planes) and reacts to benzaldehyde only when these sites are liberated. Additionally, it provides important information on the product decarbonylation, which contributes to catalyst deactivation in the absence of oxygen. Benzaldehyde desorbs intact from the sites from which CO is displaced by benzyl alcohol and does not decompose on those sites where CO is more strongly bound (envelope between 1950 and 1700 cm^{-1}). Since the signal at 1853 cm^{-1} observed during benzyl alcohol dehydrogenation on the untreated Pd catalyst (Fig. 2a) resembles the feature observed during the same reaction on the catalyst pre-equilibrated with CO (Fig. 3a), product decarbonylation occurs preferentially on such sites. These sites are predominantly hollow sites on (111) planes.

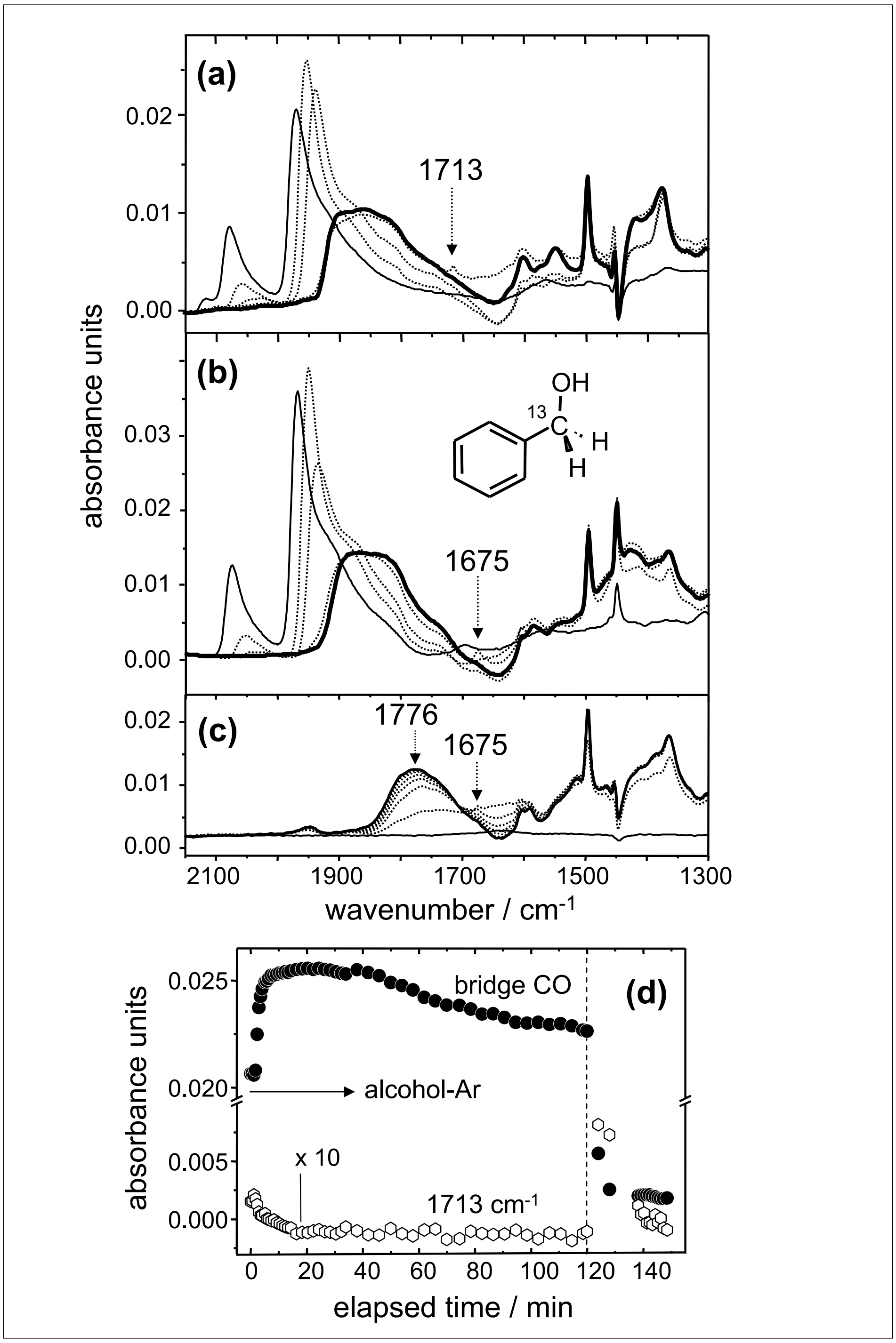

Fig. 3. ATR-IR spectra of a solution of (a) benzyl alcohol and (b) ^{13}C-benzyl alcohol under dehydrogenation conditions (Ar) on reduced Pd/Al$_2$O$_3$ pre-equilibrated with CO (1 h). Bold spectra represent the end of the experiments (*ca.* 2 h after admission of the alcohol solution). Dotted spectra are intermediate spectra taken at approximately similar time on stream. (c) Spectra of ^{13}C-benzyl alcohol dehydrogenation obtained under identical conditions to those shown in Fig. 2. The bold spectrum represents the last spectrum collected during dehydrogenation. The signals at 1776 and 1675 cm^{-1} are due to ^{13}CO and ^{13}C-benzaldehyde. (d) Time dependence of the signal of bridge CO (initially at 1968 cm^{-1}) and of that at 1713 cm^{-1} (dissolved benzaldehyde) in the experiment shown in (a). The vertical dash line indicates the onset of benzyl alcohol dehydrogenation. Conditions: $C_{alcohol}$ = 20 mM; 4 mg catalyst; cyclohexane solvent; 50 °C; liquid flow rate = 0.6 ml/min.

Fig. 4 provides a cartoon summarizing the present findings. Benzyl alcohol dehydrogenation is found to be rather structure insensitive and therefore occurs indiscriminately on all Pd sites. Product decarbonylation is favored on (111) planes, whereas the product desorption occurs from (100)

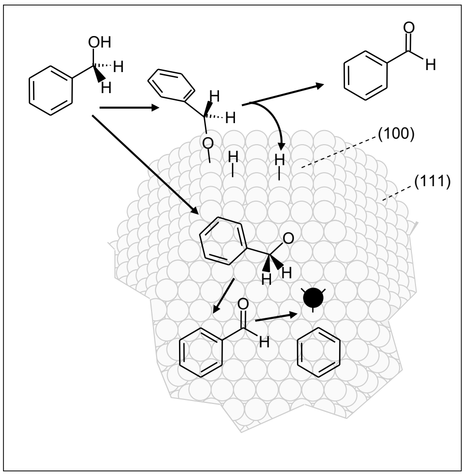

Fig. 4. Artist's view of the structural dependence of the oxidative dehydrogenation of benzyl alcohol on an ideal cubo-octahedron Pd crystallite. Only dehydrogenation on edges and (111) planes is represented for clarity. The black dot represents CO on hollow sites (top view). (Reproduced with permission from ref. [8])

planes and defects. It should be noted that these sites can also be simultaneously active for the other side reactions observed in the complex mechanism of benzyl alcohol oxidation on Pd/Al_2O_3.[3]

Bismuth Promotion

Our findings provide a reasonable explanation why supported Pd catalysts promoted by bismuth or lead are the most efficient industrial catalysts for alcohol oxidation.[12] Pd-Bi and Pt-Bi catalysts are characterized by Bi adatoms or agglomerates deposited selectively on the noble metal particles.[8,13,14] Comparison of the ATR-IR spectra recorded under dehydrogenation (Ar) and oxidative (air) conditions on Pd/Al_2O_3 and $Pd\text{-}Bi/Al_2O_3$ indicate that the influence of Bi on the reaction network is in fact remarkable. $Pd\text{-}Bi/Al_2O_3$ exhibits an almost negligible amount of CO and less intense benzoate features already under dehydrogenation conditions (Fig. 5a). Bi clearly inhibits product decarbonylation and product oxidation to benzoic acid, therefore improving selectivity. Careful inspection of the spectra also indicates that the intensity of the signal at 1713 cm^{-1} is comparable on both materials under dehydrogenation conditions.

In the presence of air, the benzoate species are again formed less abundantly on the promoted catalyst. Interestingly, the signal at 1713 cm^{-1} appears stronger on $Pd\text{-}Bi/Al_2O_3$ (arrow in Fig. 5b) and decreases after reaching a maximum although a broader window of activity is observed compared to Pd/Al_2O_3.

The data in Fig. 5 reveal that Bi-promotion better regulates the oxygen supply to the active Pd surface favoring activity in the presence of oxygen, and both selectivity and efficiency in the absence and in the presence of oxygen. Bi is in fact able to reoxidize before Pd, therefore prolonging the time the noble metal remains in the reduced state[4] and active.

The almost complete absence of adsorbed CO in the presence of Bi under dehydrogenation conditions suggests that the promoter inhibits benzaldehyde decarbonylation. This observation supports the assignment of the activity of Pd(111) planes towards product decarbonylation. Bi is probably selectively deposited on (111) planes therefore suppressing product decarbonylation.

Conclusions

In conclusion, *in situ* ATR-IR spectroscopy combined with selective site blocking by co-adsorbed CO and isotope labeling allowed us to discriminate the different sites active in the liquid-phase oxidative dehydrogenation of benzyl alcohol on Pd/Al_2O_3. Alcohol dehydrogenation to the carbonyl product occurs on virtually all exposed Pd sites. However, some of these sites (bridge sites) release the intact product and are liberated for adsorption of the reactant, whereas other sites (three-fold or hollow) promote product degradation (decarbonylation) and are probably distributed on (111) planes. These sites are selectively blocked by the Bi promoter that therefore inhibits product decarbonylation among other reactions.

The structure sensitivity of aldehyde decarbonylation implied by the present results confirms previous UHV studies, which attributed the apparent structure sensitivity of alcohol reactions on Pd to the different stability of the product on different surfaces.

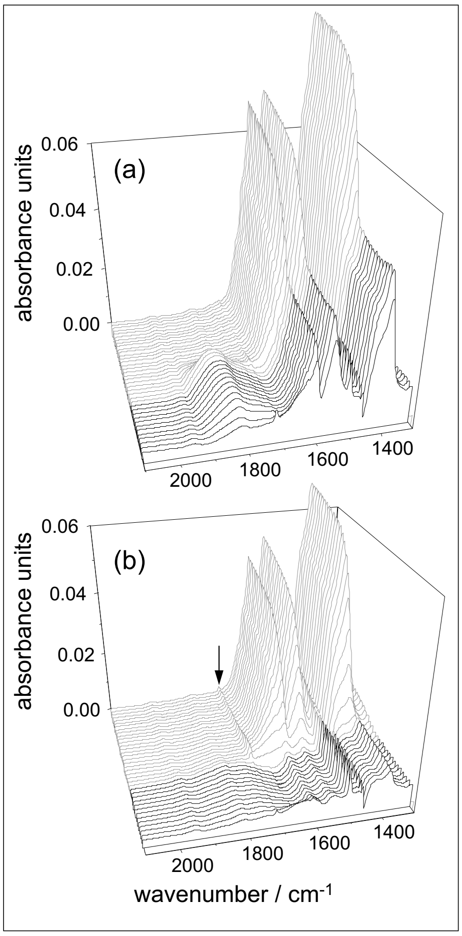

Fig. 5. ATR-IR spectra collected during oxidative dehydrogenation of benzyl alcohol on (a) Pd/Al_2O_3 and (b) $Pd\text{-}Bi/Al_2O_3$ performed under identical experimental conditions. Dark and grey spectra indicate dehydrogenation and oxidative conditions, respectively. The arrow highlights the signal of dissolved benzaldehyde. Conditions: $C_{alcohol}$ = 20 mM; 4 mg catalyst; cyclohexane solvent; 50 °C; liquid flow rate = 0.6 ml/min.

Acknowledgements

The authors acknowledge the financial support from the Foundation Claude and Giuliana. C. M. thanks for a scholarship from the University of Milan.

Received: December 18, 2006

---

[1] T. Mallat, A. Baiker, *Chem. Rev.* **2004**, *104*, 3037.
[2] T. Bürgi, M. Bieri, *J. Phys. Chem. B* **2004**, *108*, 13364.
[3] C. Keresszegi, D. Ferri, T. Mallat, A. Baiker, *J. Phys. Chem. B* **2005**, *109*, 958.
[4] C. Keresszegi, J.-D. Grunwaldt, T. Mallat, A. Baiker, *J. Catal.* **2004**, *222*, 268.
[5] N. J. Harrick, 'Internal Reflection Spectroscopy', Interscience Publishers, New York, **1967**.
[6] T. Bürgi, A. Baiker, *Adv. Catal.* **2006**, *50*, 227.
[7] T. Bürgi, R. Wirz, A. Baiker, *J. Phys. Chem. B* **2003**, *107*, 6774.
[8] D. Ferri, C. Mondelli, F. Krumeich, A. Baiker, *J. Phys. Chem. B* **2006**, *110*, 22982.
[9] T. Lear, R. Marshall, J. A. Lopez-Sanchez, S. D. Jackson, T. M. Klapötke, M. Bäumer, G. Rupprechter, H. J. Freund, D. Lennon, *J. Chem. Phys.* **2005**, *123*, 174706.
[10] S. Schauermann, J. Hoffmann, V. Johanek, J. Hartmann, J. Libuda, H. J. Freund, *Angew. Chem. Int. Ed.* **2002**, *41*, 2532.
[11] J. Xu, P. N. Henriksen, J. T. Yates, *Langmuir* **1994**, *10*, 3663.
[12] M. Besson, P. Gallezot, *Catal. Today* **2000**, *57*, 127.
[13] C. Keresszegi, T. Mallat, J. D. Grunwaldt, A. Baiker, *J. Catal.* **2004**, *225*, 138.
[14] P. Rodriguez, J. Solla-Gullon, F. J. Vidal-Iglesias, E. Herrero, A. Aldaz, J. M. Feliu, *Anal. Chem.* **2005**, *77*, 5317.